Giant primary hepatic osteosarcoma: A rare case report and review of the literature

Haoliang Zhu[1,2] **MD,**
Hangzhe Sun[1,2] **MD,**
Tianyun Zhang[1,2] **MD,**
Yu Chen[3] **MD,**
Siqi Wang[1*] **PhD**

1. Department of Nuclear Medicine, Sir Run Run Shaw Hospital, Zhejiang University School of Medicine, Hangzhou 310000, China
2. The First Clinical Medical College, Wenzhou Medical University, Wenzhou, Zhejiang 325035, China
3. National Clinical Research Center for Ocular Diseases, Eye Hospital, Wenzhou Medical University, Wenzhou, China

Keywords: Primary hepatic osteosarcoma - Extraskeletal osteosarcoma - Liver neoplasms - SATB2 protein - Radiology

Corresponding author:
Siqi Wang PhD,
Department of Nuclear Medicine, Sir Run Run Shaw Hospital, Zhejiang University School of Medicine, Hangzhou 310000, China
B2418173@zju.edu.cn

Received:
6 August 2025
Accepted:
10 January 2026

Abstract

Objective: Primary hepatic extraskeletal osteosarcoma (PHOS) is an extremely rare and aggressive malignant tumor originating in the liver with no primary skeletal lesion. Less than 1% of all extraskeletal osteosarcomas occur in the liver, often presenting as a large abdominal mass with poor prognosis. **Case Presentation:** We report a rare case of a 64-year-old man diagnosed with a giant PHOS (163×128×160mm) accompanied by pulmonary and lymph node metastases. Multimodal imaging (magnetic resonance imaging (MRI), computed tomography (CT), bone scintigraphy, positron emission tomography (PET)/CT demonstrated a heterogeneous hepatic mass with extensive calcifications, rim enhancement, restricted diffusion, and elevated fluorine-18-fluorodeoxyglucose (^{18}F-FDG) uptake. Histopathological analysis confirmed the diagnosis, showing atypical mesenchymal cells producing osteoid matrix with strong special AT-rich sequence-binding protein 2 (SATB2) positivity and negative epithelial markers. **Discussion:** Imaging characteristics and immunohistochemical profiling were crucial in differentiating PHOS from hepatocellular carcinoma and metastatic osteosarcoma. The case supports the metaplasia theory of PHOS pathogenesis and highlights its radiologic-pathologic correlation, especially the "cloud-like" enhancement on imaging corresponding to unmineralized osteoid and vascular proliferation. **Conclusion:** This case highlights the diagnostic challenge and clinical significance of PHOS. Comprehensive imaging and pathological evaluation are essential for accurate diagnosis. Due to its rarity and aggressiveness, PHOS requires individualized management strategies, typically involving surgery and adjuvant therapies despite limited evidence-based guidelines.

Hell J Nucl Med 2026; 29(1): 42-47 *Epub ahead of print: 7 April 2026* *Published online: 30 April 2026*

Introduction

Extraskeletal osteosarcoma (ESOS) is a rare malignant tumor that arises in soft tissues without skeletal involvement. Primary hepatic ESOS constitutes an exceptionally rare subtype. Only dozens of primary hepatic osteosarcoma (PHOS) cases have been documented worldwide, accounting for less than 1% of all ESOS [1]. Primary hepatic osteosarcoma typically presents a rapidly enlarging abdominal mass, carrying a dismal prognosis with a median survival under six months [1-3]. The diagnosis necessitates both histopathological verification and corroborative imaging findings, with mandatory exclusion of metastatic osteosarcoma arising from primary skeletal lesions. Here, we report a 64-year-old male with a giant PHOS and concomitant pulmonary metastases.

Case presentation

A 64-year-old man presented to the hospital following the detection of a mass in the abdomen's right upper quadrant during a routine physical examination two days prior. Five days later, he was hospitalized with nausea, vomiting, heartburn and persistent hiccups. On admission, the patient denied abdominal pain and fever in a stable condition. Laboratory tests showed a markedly elevated CA19-9 level (1905.3kU/L) and elevated alkaline phosphatase (ALP) (554U/L).

Contrast-enhanced magnetic resonance imaging (MRI) was initially obtained to evaluate the lesion. Images demonstrate a hepatic mass measuring 163×128×160mm span-

ning both liver lobes, exhibiting infiltrative tumor borders. Representative findings are shown in Figures 1 & 2. The T2-weighted MRI demonstrates heterogeneous signal intensity with intermixed components (Figure 1A). On diffusion-weighted imaging (DWI) (b=800s/mm^2), the mass demonstrates hyperintensity indicating restricted diffusion (Figure 1B). On pre-contrast T1-weighted imaging (Figure 1E), the mass appears hypointense. During the arterial phase (Figure 1F), the mass exhibits heterogeneous peripheral rim enhancement. In the portal venous phase (Figure 1G), it is demonstrated progressive centripetal enhancement. No signal drop was observed on in-phase/out-of-phase T1 imaging (Figure 1C-D) indicating the absence of fatty tissue in the mass. Calcifications were better delineated on computed tomography (CT) compared to MRI. There were non-enhancing areas internally in the mass on both enhanced MRI and CT imaging.

Whole-body bone scintigraphy was performed 3 hours after the intravenous injection of 20-25mCi (740-925MBq) of technetium-99m-methylene diphosphonate (^{99m}Tc-MDP). Heterogeneous radiotracer distribution in the neck and sternum (usually physiological). Uptake of the tracer in the liver indicates extraosseous uptake in the tumor (Figure 3A).

Positron emission tomography (PET)/CT further demonstrated significantly heterogeneously increased fluorine-18-fluorodeoxyglucose (^{18}F-FDG) uptake in the hepatic mass with a maximum standardized uptake value (SUVmax) value of 20.99, while no tracer uptake is observed in the central region of the mass (Figure 3C). An enlarged and hypermetabolic lymph node in the hepatogastric space indicates lymph node metastasis. Multiple metastatic nodules with elevated ^{18}F-FDG metabolism are presented in both lungs. The largest nodule among them, located in the lower right lobe,

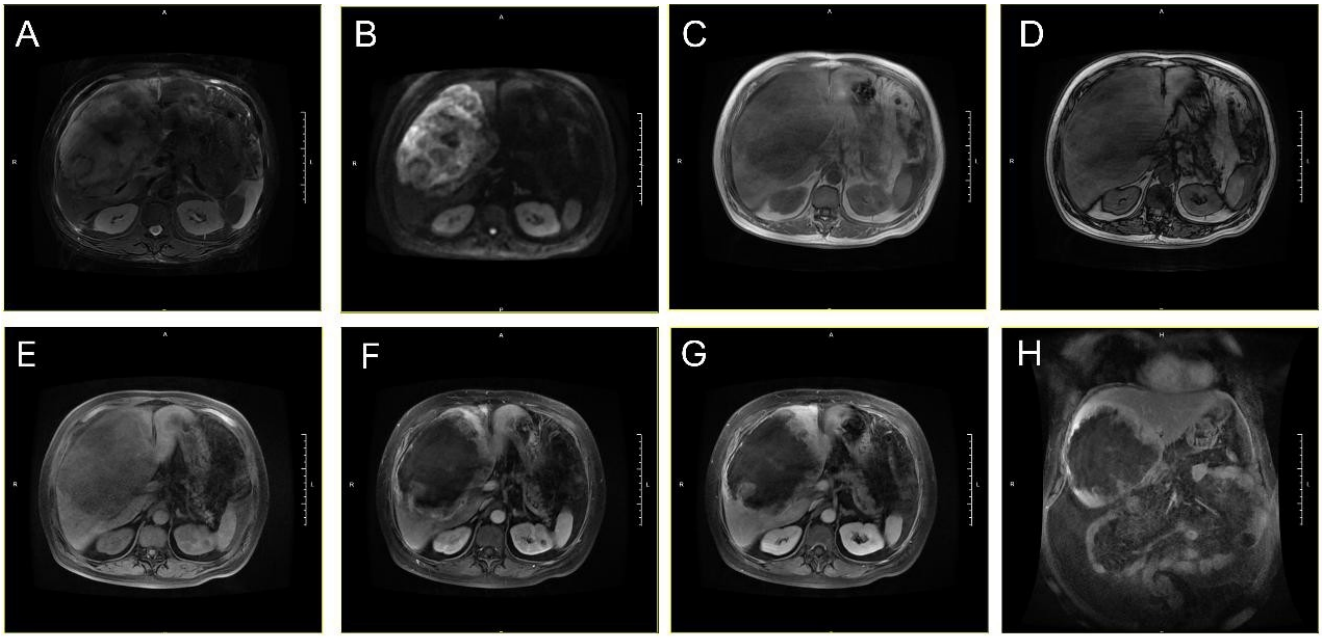

Figure 1. Non-contrast MRI. (A) T2-weighted imaging (T2WI) shows a 163×128×160mm trans-lobar mass with ill-defined margins and heterogeneous high/low signals; (B) DWI demonstrates hyperintensity (b=800); (C-D) In-phase/opposed-phase T1-weighted imaging shows no significant signal drop within the lesion. (E) Pre-contrast T1WI shows a hypointense mass; (F) Arterial phase demonstrates rim enhancement in the peripheral solid component; (G) Portal venous phase shows centripetal extension of enhancement; (H) Delayed phase reveals no enhancement in the central necrotic area.

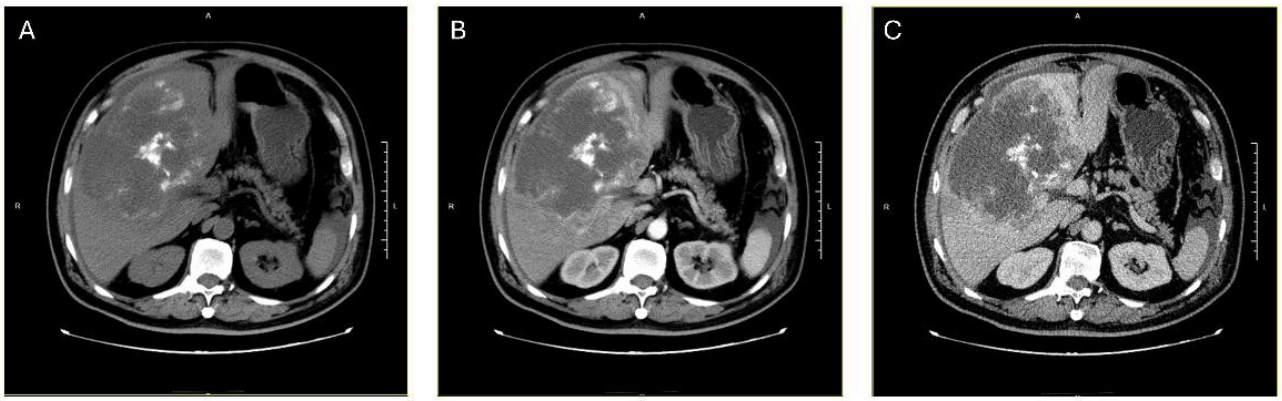

Figure 2. Contrast-enhanced CT. (A) Plain CT scan shows a 163×128×160mm heterogeneous mass with patchy calcifications; (B) Arterial phase shows marked marginal enhancement; (C) Venous phase demonstrates progressive enhancement.

measured approximately 0.76cm with a SUVmax value of 5.5 (Figure 3B). The punctate hypermetabolic foci in the midline and axillary regions on the maximum intensity projection (MIP) image are due to external tracer contamination. Apart from the afore-mentioned regions, no other substantial parenchymal lesions or abnormal radiotracer distribution were detected. The existence of hypermetabolism suggests tumor heterogeneity and highly aggressive biological behavior.

All the imaging findings suggested a primary malignant liver tumor. Consequently, the patient underwent a CT-guided liver biopsy. The collected tissue samples were sent to the pathology department for analysis and diagnosis.

The hematoxylin and eosin (HE) stained tissue section (Figure 4), exhibits pronounced heterogeneity and malignant characteristics. The cells are arranged in a disordered architecture and predominantly exhibit fusiform, polygonal, or irregular morphologies. Their nuclei are large, hyperchromatic, with an imbalanced nuclear-to-cytoplasmic ratio, distinct nucleoli, and numerous pathological mitotic figures, indicative of high proliferative activity.

Immunohistochemical staining of the liver biopsy (Figure 4) showed: Hepatocyte (–), AFP (–), CK7 (–), CK19 (–); the key marker special AT-rich sequence-binding protein 2 (SATB2) exhibited strong positive expression (+). CK-pan was only weakly positive in limited areas, and epithelial marker (CK-high) was negative. Consequently, the diagnosis of PHOS was confirmed based on radiology, nuclear medicine and pathological findings.

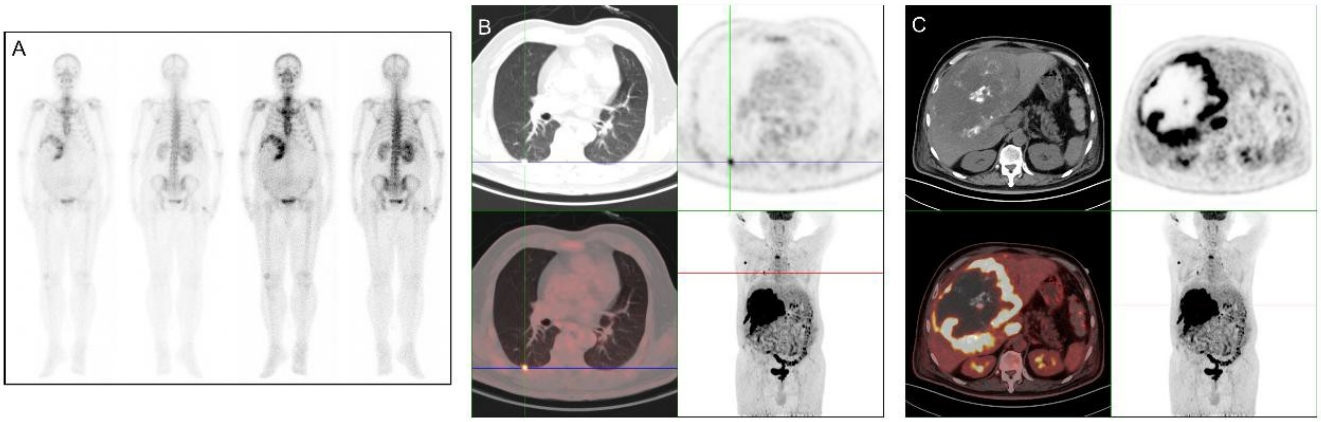

Figure 3. (A) Whole-body bone scintigraphy. Focal radiotracer uptake is increased in the liver. Physiological uptake is in the cervical and sternal regions. PET/CT. (B) Lung window shows multiple ^{18}F-FDG-avid pulmonary nodules (SUVmax=5.5); (C) Liver window demonstrates a mass with high ^{18}F-FDG uptake (SUVmax=20.99). The red arrow shows lymph node metastasis. There are some radioactive contamination spots in the right axilla and anterior chest area.

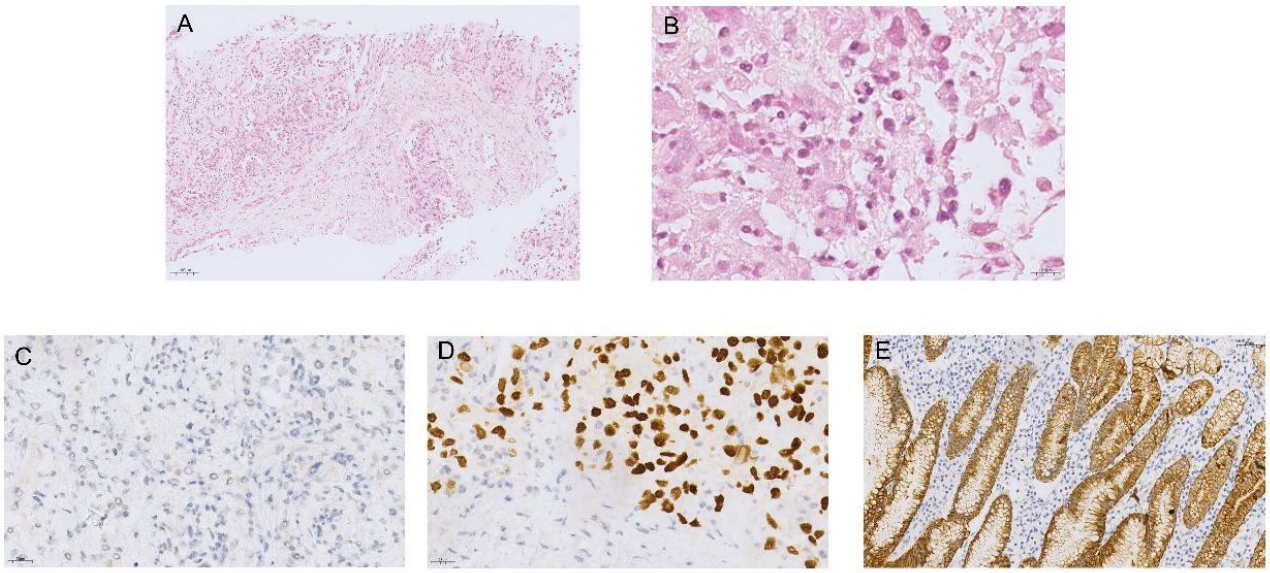

Figure 4. Histopathological and immunohistochemical features of primary hepatic osteosarcoma. (A) Low-power view (×10, H&E) showing disrupted hepatic parenchyma with infiltrating spindle-to-polygonal tumor cells embedded in lace-like osteoid matrix (yellow arrows). (B) High-power view (×80, H&E) revealing hyperchromatic atypical nuclei with irregular contours and pathological mitoses (red arrow). C) Alpha-fetoprotein mmunohistochemistry (×40): Negative tumor staining (positive internal hepatocyte control). (D) SATB2 immunohistochemistry (×40): Strong nuclear positivity in tumor cells. (E) CK- pan immunohistochemistry (×20): Focal weak cytoplasmic positivity

Discussion

Primary hepatic osteosarcoma has a poor prognosis due to its invasive growth pattern, early blood-borne spread, and frequent recurrences [4]. Patients usually report vague symptoms like abdominal pain, fatigue and loss of appetite which reflect the tumor's rapid growth and high chance of spreading (lung metastases occur in 37%-80% of cases) [5]. Two predominant mechanistic hypotheses have been proposed to explain the pathogenesis of PHOS [6]. The tissue residual theory posits malignant transformation of embryonically derived mesenchymal progenitor cells in soft tissues, while the metaplasia theory suggests aberrant differentiation of interstitial fibroblasts into osteoblasts/chondroblasts under specific stimuli (like chronic inflammation or radiation). The metaplasia theory currently predominates, as it more plausibly explains ESOS occurrence in liver devoid of inherent osteogenic potential, implicating acquired cellular reprogramming rather than developmental remnants [7, 8].

Due to its rarity, PHOS presents a significant diagnostic dilemma, often mimicking common hepatic lesions. Accurately distinguishing PHOS relies heavily on a multimodal approach integrating distinctive radiological patterns with specific immunohistochemical profiles (such as SATB2). A review of the literature reveals that PHOS predominantly affects older adults and is associated with a dismal prognosis. The following table summarizes key clinical characteristics of PHOS cases reported in the literature, highlighting the rarity of long-term survival and the typically large tumor burden at presentation, which aligns with the giant mass observed in our case.

Primary hepatic osteosarcoma typically appears as an ill-defined heterogeneous mass with irregular calcifications or ossifications in cotton-like, ivory-like, or speculated patterns

Table 1: *Summary of reported cases of primary hepatic osteosarcoma.*

Author (Year)	Age/Sex	Tumor location/ Size	Key clinical/Pathological features	Outcome	Reference (Citation)
Maynard et al. (1969)	52/M	Right lobe/Massive (1.7 kg)	Associated with hemochromatosis and cirrhosis. First reported case.	Died (3 weeks)	[9]
Sumiyoshi et al. (1971)	71/M	Right lobe/25cm	Autopsy case; cirrhosis present.	Died (2 months)	[10]
Von et al. (1987)	73/F	Right lobe/10cm	No cirrhosis.	Died	[11]
Govender et al. (1998)	72/M	Right lobe/25cm	HBV negative; presented with abdominal pain.	Died (4 months)	[12]
Park et al. (2009)	60/F	Right lobe/15cm	Giant mass similar to present case; aggressive recurrence.	Died (2.5 months)	[13]
Nawabi et al. (2009)	19/F	Right lobe/15cm	Rare young case; treated with resection + chemotherapy.	Alive (>36 months)	[14]
Tamang et al. (2016)	47/M	Right lobe/11cm	HBV positive.	Alive (3 months follow-up)	[15]
Yu et al. (2018)	70/M	Right lobe/8.5cm	History of abdominal trauma; Vimentin+, CD10+.	Died (4 months)	[16]
Zhang et al. (2021)	62/M	Exophytic (Liver-kidney space)/7.8cm	Exophytic growth pattern; treated with surgery + chemo.	Alive (No recurrence)	[17]
Di et al. (2023)	76/M	Right lobe/Giant	Relapsed case; rapid recurrence (48 days post-op).	Died (Post-op failure)	[18]
Yang et al. (2024)	Adult/F	Right lobe/Mass	Non-calcified variant (rare); rare absence of typical calcification.	Died (8.5 months)	[19]

on CT [20]. The pathological mechanisms of calcification and ossification in osteosarcoma mainly involve three interrelated processes [21, 22]: Abnormal osteogenic differentiation of tumor cells, dysregulation of the tumor microenvironment, and activation of ectopic bone formation signaling pathways. From a radiologic-pathologic correlation perspective, the characteristic high-density calcifications observed on CT imaging typically represent mineralization of mature lamellar bone [23-25]. On contrast-enhanced CT, it demonstrates peripheral enhancement in the arterial phase and characteristic centripetal "cloud-like" enhancement in portal phase. During scans with contrast dye, the tumor's edges light up first, then show a special "cloud-like" pattern as the dye spreads inward [26, 27]. These imaging features reflect the underlying pathological process of disorganized bone matrix production by malignant cells combined with aberrant vascular proliferation. On MRI, it shows hypo-to-isointense signal on T1WI and heterogeneous hyperintensity on T2WI, with similar enhancement patterns to CT. Restricted diffusion is observed in solid components on DWI. The central portion demonstrates no enhancement, consistent with necrosis or hemorrhage [28]. This case demonstrates imaging features consistent with the above description.

Notably, PHOS requires differentiation from two key entities: hepatocellular carcinoma (HCC) with ossification and metastatic osteosarcoma. Hepatocellular carcinoma with ossification is more common in patients with cirrhosis or chronic hepatitis, typically exhibiting focal calcifications/ossifications at the tumor periphery or necrotic areas and showing the classic "wash-in and wash-out" enhancement pattern on imaging, often accompanied by elevated AFP. Primary hepatic osteosarcoma demonstrates more extensive ossification, whereas HCC presents with smaller ossified areas and more characteristic enhancement behavior. The two can be differentiated based on imaging features combined with clinical context. As for the differentiation of metastatic osteosarcoma, whole-body bone scintigraphy and PET/CT play important roles in ruling out bone lesions. In this case, the whole-body bone scintigraphy indicates ectopic osteoid formation in the hepatic tumor with concomitant exclusion of osseous lesions (Figure 4). Positron emission tomography/CT combines the anatomical structure on CT and functional information on PET, which can not only rule out bone lesions more comprehensively, but also show the extent of metastasis [9]. In this case, it rules out bone lesions and shows lung metastasis, but there are some radioactive contamination spots in the right axilla and anterior chest area (Figure 3C).

Pathologically, it is characterized by direct osteoid matrix production by atypical mesenchymal cells, confirmed by SATB2/vimentin positivity and epithelial marker negativity. Diagnosis requires histopathological confirmation of osteoid-producing malignant cells and SATB2 immunopositivity, alongside exclusion of primary skeletal lesions [29, 30].

In addition, the focal cytokeratin (CK) expression observed in our osteosarcoma case aligns with the emerging concept of epithelial-mesenchymal plasticity demonstrated across organ systems. Liu et al. (2004) revealed that normal biliary epithelial cells can aberrantly express hepatocyte markers (AFP/Albumin) under specific conditions, while Demirkesen et al. (1995) documented hybrid CK patterns (e.g., CK5/6+ CK19) in cutaneous adnexal tumors - both phenomena mirroring our finding of limited CK-pan positivity in mesenchymal-derived osteosarcoma [31, 32]. This transient epithelial marker expression likely reflects tumor cell dedifferentiation reactivating developmental pathways. Crucially, just as biliary CK19+ cells maintain mesenchymal functions and sweat gland tumors retain ductal architecture despite aberrant CK7 expression, our case's dominant SATB2 positivity and osteoid production confirm osteogenic lineage despite focal CK reactivity. These cross-tissue parallels underscore that limited CK expression in sarcomas represents biological plasticity rather than true epithelial differentiation, classifying such cases as osteosarcoma when supported by definitive mesenchymal markers.

Treatment involves radical surgery combined with adjuvant chemoradiation, though these show limited efficacy against distant metastasis [6]. Because PHOS is so rare, no standard treatment guidelines exist. Aggressive surgical intervention remains the principal treatment strategy; nevertheless, clinical outcomes frequently prove suboptimal [30, 33, 34].

In conclusion, PHOS is an extremely rare (less than 1% of all non-osseous osteosarcomas occur in the liver) and aggressive malignancy. The unique clinical value of our case lies in the giant mass of PHOS (163mm) exceeding the average size of similar cases (10cm). Multi-modality imaging including CT, MRI, bone scintigraphy and PET/CT provided specific diagnostic evidence. Definitive diagnosis ultimately relies on pathological examination and immunohistochemical analysis. Due to its rarity and aggressiveness, PHOS requires individualized management strategies, typically involving surgery and adjuvant therapies, despite limited evidence-based guidelines.

The authors declare that they have no conflicts of interest

Bibliography

1. Di QY, Long XD, Ning J et al. Relapsed Primary Extraskeletal Osteosarcoma of Liver: A Case Report and Review of Literature. *World J Clin Cases* 2023; 11(3): 662-8.
2. Yang C, Qin LH, Chen PY et al. A Case of Non-Calcified Intrahepatic Primary Osteosarcoma: A Case Report and a Literature Review. *Curr Med Imaging* 2024; 20: e15734056326695.
3. Tamang TG, Shuster M, Chandra AB. Primary Hepatic Osteosarcoma: A Rare Cause of Primary Liver Tumor. *Clin Med Insights Case Rep* 2016; 9: 31-3.
4. Allan CJ, Soule EH. Osteogenic Sarcoma of the Somatic Soft Tissues. Clinicopathologic Study of 26 Cases and Review of Literature. *Cancer* 1971; 27(5): 1121-33.
5. Zhang J, He X, Yu W et al. Primary Exophytic Extraskeletal Osteosarcoma of the Liver: A Case Report and Literature Review. *Risk Manag Healthc Policy* 2021; 14: 1009-14.
6. Patnaik AK, Liu S, Johnson GF. Extraskeletal Osteosarcoma of the Liver in a Dog. *J Small Anim Pract* 1976; 17(6): 365-70.
7. Cheng M, Jin J, Zhang D et al. Mettl3 Obstructs Vascular Smooth Muscle Cells Osteogenic Reprogramming by Methylating Runx2 in Chronic Kidney Disease. *Commun Biol* 2025; 8(1): 582.
8. Wang YC, Wang ZJ, Zhang C, Ning BF. Cell Reprogramming in Liver with Potential Clinical Correlations. *J Dig Dis* 2022; 23(1): 13-21.

9. Maynard J.H, Fone D.J. Haemochromatosis with osteogenic sarcoma in the liver. *Med J Aust* 1969; 2(25): 1260-3.
10. Sumiyoshi A, Niho Y. Primary osteogenic sarcoma of the liver-report of an autopsy case. *Acta Pathol Jpn* 1971; 21(2): 305-12.
11. von Hochstetter A.R, Hättenschwiler J, Vogt M. Primary osteosarcoma of the liver. *Cancer* 1987; 60(9): 2312-7.
12. Govender D, Rughubar K.N. Primary hepatic osteosarcoma: case report and literature review. *Pathology* 1998; 30(3): 323-5.
13. Park SH, Choi SB, Kim WB, Song TJ. Huge primary osteosarcoma of the liver presenting an aggressive recurrent pattern following surgical resection. *J Dig Dis* 2009; 10(3): 231-5.
14. Nawabi A, Rath S, Nissen N et al. Primary hepatic osteosarcoma. *J Gastrointest Surg* 2009; 13(8): 1550-3.
15. Tamang TG, Shuster M, Chandra AB. Primary Hepatic Osteosarcoma: A Rare Cause of Primary Liver Tumor. *Clin Med Insights Case Rep* 2016; 9: 31-3.
16. Yu L, Yang SJ. Primary Osteosarcoma of the Liver: Case Report and Literature Review. *Pathol Oncol Res* 2020; 26(1): 115-20.
17. Zhang J, He X, Yu W et al. Primary Exophytic Extraskeletal Osteosarcoma of the Liver: A Case Report and Literature Review. *Risk Manag Healthc Policy* 2021; 14: 1009-14.
18. Di QY, Long XD, Ning J et al. Relapsed primary extraskeletal osteosarcoma of liver: A case report and review of literature. *World J Clin Cases* 2023; 11(3): 662-8.
19. Yang C, Qin LH, Chen PY et al. A Case of Non-calcified Intrahepatic Primary Osteosarcoma: A Case Report and a Literature Review. *Curr Med Imaging* 2024; 20: e15734056326695.
20. Hoch M, Ali S, Agrawal S et al. Extraskeletal Osteosarcoma: A Case Report and Review of the Literature. *J Radiol Case Rep* 2013; 7(7): 15-23.
21. Baroncelli M, van der Eerden BCJ, Chatterji S et al. Human Osteoblast-Derived Extracellular Matrix with High Homology to Bone Proteome Is Osteopromotive. *Tissue Eng Part A* 2018; 24(17-18): 1377-89.
22. Wang Y, Sun JC, Wang HB et al. Acvr1-Knockout Promotes Osteogenic Differentiation by Activating the Wnt Signaling Pathway in Mice. *J Cell Biochem* 2019; 120(5): 8185-94.
23. Aliyev A, Ekin Ö, Bitik O et al. A Novel Method of Neo-Osseous Flap Prefabrication: Induction of Free Calvarial Periosteum with Bioactive Glass. *J Reconstr Microsurg* 2018; 34(5): 307-14.
24. Rossi F, Rydzyk MM, Barba L et al. Insights into the Osteosarcoma Microenvironment: Multiscale Analysis of Structural and Mineral Heterogeneity. *Acta Biomater* 2025; 199: 193-201.
25. Zhan Y, Deng B, Wu H et al. Biomineralized Composite Liquid Crystal Fiber Scaffold Promotes Bone Regeneration by Enhancement of Osteogenesis and Angiogenesis. *Front Pharmacol* 2021; 12: 736301.
26. Jiang L, Xie L, Wu Z et al. Imaging Features of Hepatic Angiosarcoma: Retrospective Analysis of Two Centers. *BMC Cancer* 2024; 24(1): 1191.
27. Li L, Liu W, Wen R, Jin K. Computed Tomography Imaging and Clinical Features of Congenital Hepatoblastoma: A Retrospective Analysis. *Medicine (Baltimore)* 2020; 99(31): e21174.
28. Puac-Polanco P, Zakhari N, Miller J et al. Diagnostic Accuracy of Centrally Restricted Diffusion Sign in Cerebral Metastatic Disease: Differentiating Radiation Necrosis from Tumor Recurrence. *Can Assoc Radiol J* 2023; 74(1): 100-9.
29. Kraft GH. Foreword: Radiculopathy. *Phys Med Rehabil Clin N Am* 2011; 22(1): xi-xii.
30. Nystrom LM, Reimer NB, Reith JD et al. The Treatment and Outcomes of Extraskeletal Osteosarcoma: Institutional Experience and Review of the Literature. *Iowa Orthop J* 2016; 36: 98-103.
31. Liu C, Schreiter T, Dirsch O et al. Presence of Markers for Liver Progenitor Cells in Human-Derived Intrahepatic Biliary Epithelial Cells. *Liver Int* 2004; 24(6): 669-78.
32. Demirkesen C, Hoede N, Moll R. Epithelial Markers and Differentiation in Adnexal Neoplasms of the Skin: An Immunohistochemical Study Including Individual Cytokeratins. *J Cutan Pathol* 1995; 22(6): 518-35.
33. Berner K, Bjerkehagen B, Bruland Ø S, Berner A. Extraskeletal Osteosarcoma in Norway, between 1975 and 2009, and a Brief Review of the Literature. *Anticancer Res* 2015; 35(4): 2129-40.
34. Federman N, Bernthal N, Eilber FC, Tap WD. The Multidisciplinary Management of Osteosarcoma. *Curr Treat Options Oncol* 2009; 10(1-2): 82-93.